

Crystallization of gels in the $\text{SiO}_2\text{-ZrO}_2\text{-B}_2\text{O}_3$ system

F. LIU

State Key Laboratory of Solidification Processing, Northwestern Polytechnical University, Xi'an, Shaanxi 710072, People's Republic of China
E-mail: caoyang77@263.net

X. F. GUO

College of Material Science and Engineering, Xi'an University of Technology, Xi'an, Shaanxi 710048, People's Republic of China

G. C. YANG

State Key Laboratory of Solidification Processing, Northwestern Polytechnical University, Xi'an, Shaanxi 710072, People's Republic of China

The preparation of glasses from gels in the ternary system of $\text{SiO}_2\text{-ZrO}_2\text{-B}_2\text{O}_3$ has been investigated. The crystallization character of ZrO_2 particles and high-temperature structure stability in the $\text{SiO}_2\text{-ZrO}_2\text{-B}_2\text{O}_3$ gels were analyzed. The effect of B_2O_3 as the inhibitor of crystallization was illustrated. Finally, the result that the purified DD3 single crystal superalloy melt can retain high undercooling in the $\text{SiO}_2\text{-ZrO}_2\text{-B}_2\text{O}_3$ coating mold indicates that the coating has an ideal non-catalytic nucleation property.

© 2001 Kluwer Academic Publishers

1. Introduction

Rapid solidification of highly undercooled melt has been given more and more emphasis in condensational physics and materials research fields [1, 2], because of the fact that the ultrafine solidification structures were obtained through this process [3, 4]. However, this kind of rapid solidification is carried out under the condition of levitation melting or in high purity quartz glass crucible [1, 3], and it is impossible to prepare directly bulk rapidly solidified materials because of the limitation of melt volume and the nucleation catalysis of mold. Bulk rapidly solidified materials could be prepared only by pouring the highly undercooled melt into non-catalytic coating mould, provided that the undercooling of the melt is partly or completely retained [3]. But effective and cheap way for the preparation of non-catalytic nucleation coating is not available yet, accordingly, the research of bulk rapidly solidified materials is far from being settled. The recent research [3, 10] showed that the undercooling retained from the highly undercooled melt in the non-catalytic coating mold depends on the structure and high-temperature structure stability of the coating. If coating keeps stable vitreous or less crystalline trend at high temperature, high undercooling can be obtained in the coating mold. Therefore, the research and preparation of the glass-lined coating with structure stability at high temperature is decisive to the preparation of bulk rapidly solidified materials. In 1981, by using dynamic undercooling which means that a temperature gradient of about $10^\circ\text{C}/\text{cm}$ is maintained within the melt during the cooling process, B. Lux [4] investigated the capability

of various mould materials in nucleation inhibition. A large undercooling up to 191 K was obtained in Zircon (ZrSiO_4) mold, which is a kind of ZrO_2 (Zirconia)-containing ceramic. Zirconia and silica has been well established by sun [5] to be both glass formers and intermediates in relation to its bond strengths and glass formation capabilities. Zirconia is expected to incorporate in the structure of silica networks to form a multicomponent glass. Glass formation in the silica-zirconia system deserves intensive study because of its importance in the refractory industries. The glass in this system can be chemically stable, refractory, of high modulus and excellent toughness. However, it is rather difficult to prepare with conventional melting techniques because of its high melting temperature and the presence of an extensive miscibility gap. Consequently, recent attempts have been concentrated on the preparation of this glass by the calcination of gel, and some encouraging results have been reported [6, 7]. Meanwhile, Gels and glasses of the $\text{B}_2\text{O}_3\text{-SiO}_2$ system have been widely researched by several authors [8, 9]. B_2O_3 acts as an inhibitor of the crystallization trend in silica gels, according to Jabra *et al.* [9], but the correspondent research work of $\text{SiO}_2\text{-ZrO}_2\text{-B}_2\text{O}_3$ (symbolized as Si-Zr-B) glass or ceramic has not been reported yet.

In this paper, we aimed to clarify the following points: (1) the structural changes associated with crystallization of gels in the systems, (2) the effect of B_2O_3 as the inhibitor of crystallization in the $\text{SiO}_2\text{-B}_2\text{O}_3$ and $\text{SiO}_2\text{-ZrO}_2\text{-B}_2\text{O}_3$ systems, (3) the non-catalytic nucleation property of the $\text{SiO}_2\text{-ZrO}_2\text{-B}_2\text{O}_3$ coating.

TABLE I Composition of gel sample

Samples	Calculated composition (wt%)
a	100 SiO ₂
b	90 SiO ₂ + 10 ZrO ₂
c	80 SiO ₂ + 20 ZrO ₂
d	97SiO ₂ + 3 B ₂ O ₃
e	87 SiO ₂ + 10 ZrO ₂ + 3 B ₂ O ₃
f	78SiO ₂ + 19% ZrO ₂ + 3 B ₂ O ₃

2. Experiment procedure

2.1. Sol preparation

Six gel compositions of the SiO₂-ZrO₂-B₂O₃ system were prepared (Table I) by using tetraethylorthosilicate (TEOS) as SiO₂ source, ZrOCl₂·8H₂O as ZrO₂ source, and boric acid (H₃BO₃) as B₂O₃ source.

ZrOCl₂·8H₂O and boric acid were dissolved in ethanol and then the mixture was added with 5.65 ml H₂O. After a few minutes of vigorous stirring, a clear and homogeneous solution was obtained. Stirring was maintained for another 30 minutes after being added with TEOS. The molar ratio to water of the alkoxide molecule TEOS : H₂O was adjusted to 1 : 3 in order to avoid the precipitation of H₃BO₃ and Zr(OH)₄. Then the precursor solution was covered with a plastic sheet, sealed and placed in a forced-air stove at 35°C.

The preparation procedures of pure SiO₂ and SiO₂-B₂O₃ gel are shown in ref [10].

2.2. Gelling and heat-treatment

According to the overall gelation time of every variety of sols corresponding to their compositions, different time for reaction of hydrolyzing-condensation at 35°C was chosen to prepare different T-sol. Thereafter, the T-sols were poured onto glassboard for gelation. For the purpose of investigating the structural changes associated with the crystallization, the heat treatment was also scheduled. Once the T-gels had been dried at ambient temperature for 24 hours, they were heat treated at different temperature from ambient temperature to 1500°C. Firstly, the T-gels was heated from ambient temperature to 45°C at a heating rate of 3°C/min, and held for 2 hours, then raised it to a temperature of 500°C from 45°C at a heating rate of 2°C/min, keeping for 1 hour. Subsequently, the T-gels was heated to 850°C for glassing treatment for 1 hour. After that, placed the T-gels directly into the oven with temperature of 950, 1050, 1200, 1350, 1500°C for 30 min for structural stability analysis respectively.

After heat treatment, a philips X-ray diffractometer was used to identify the crystalline phases presented in the heat treated gels. Finely ground gel powder was placed on an aluminum disc as a substrate and nickel-filtered CuKα radiation was employed. Different thermal analysis (DTA) of the gel sample was performed using a Rigaku. Micro DTA apparatus at a heating rate of 10°C/min. Infrared (IR) spectra were recorded (in KBr pellet) using a perkin-Elmer 580 double beam IR spectrophotometer.

2.3. Undercooling measurement in the Si-Zr-B non-catalytic nucleation coating

In this experiment, sample f was chosen as the original composition of Si-Zr-B coating, the detailed procedure for the preparation of Si-Zr-B coating mold is shown in ref [11]. Thereafter, poured DD3 single crystal superalloy melt, which was first purified and then obtained high undercooling, into the Si-Zr-B coating mold under an Argon atmosphere in the high frequency heating coil. Then it was processed in a mode of the following successive cycles: melting—superheating for 2–3 min—cooling—solidification. After the high frequency power source was turned off, the alloy sample was spontaneously cooled and the cooling curve was recorded by an infrared temperature sensing system that is calibrated with a standard PtPh₃₀-PtRh₆ thermocouple.

3. Result

3.1. Stability of gel-derived Si-Zr-B glass

The stability and persistence of tetragonal zirconia in the absence or presence of matrix constraint are investigated by calcination of hydrated zirconium salt and T-gels, respectively, at various temperatures. Calcined samples are analyzed for tetragonal and monoclinic (symbolized as t and m, respectively) zirconia by X-ray diffraction (XRD). The data are plotted as a percentage of the total crystalline zirconia against temperature (Fig. 1). During the calcination of zirconium salt, the results indicate a sharp reduction in the proportion of tetragonal zirconia left between 555 and 750°C, and less than 5% remain at 1350°C. In contrast to this, almost 100% tetragonal zirconia persist up to 1350°C in the SiO₂-ZrO₂ and SiO₂-ZrO₂-B₂O₃ gel systems. Fig. 2 shows the growth of metastable t-ZrO₂ crystallites in the SiO₂-ZrO₂ and SiO₂-ZrO₂-B₂O₃ gel systems, respectively. Although the proportion of zirconia in both matrices is about 20wt%, the crystallites appear to grow at a rate faster in the SiO₂ matrix than in the SiO₂-B₂O₃ matrix. The results also infer that the growth rates of these crystallites should be very slow.

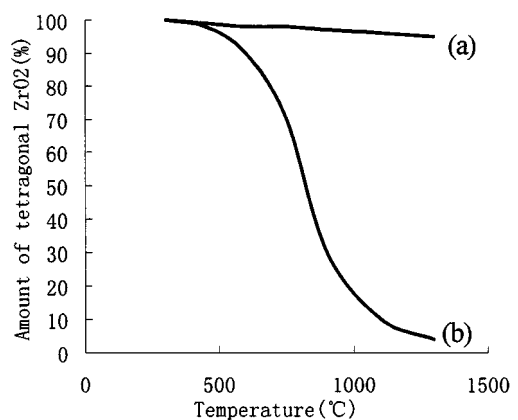


Figure 1 Variation of the amount of tetragonal ZrO₂ present in the hydrated zirconium salt (a) and the prepared gel sample f (b) as a function of temperature.

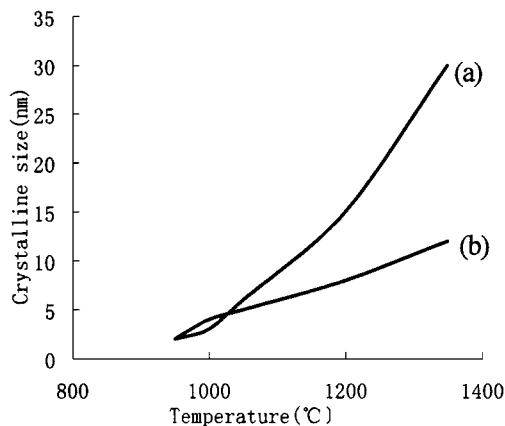


Figure 2 Growth of metastable t-ZrO₂ particles in silica (a) and silica-boron (b) matrices.

3.2. Crystallization characteristics of gels

The desiccated gels obtained by heating up to 850 °C remain glassy or amorphous as confirmed by the complete absence of crystalline phase in the XRD results (see Table II and Fig. 3). The crystallization temperatures of the various phases, particularly the zirconia phase, are sensitively dependent on the compositions of the gels. The first crystalline phase appears to be always the metastable t-ZrO₂. At higher temperature, m-ZrO₂ and cristobalite (existing solely in sample a, b and c) are detected.

The thermochemical reaction taking place and the progressive evolution of the gel with separation of crystalline phases during heat treatment have been studied by the DTA and thermogravimetric analysis (TGA) technique. The DTA and TGA curves for T-gel sample f are depicted in Fig. 4 and Fig. 5, respectively. The prominent endothermic features of the DTA curves are attributed to the desorption of physically absorbed water (100–150 °C), and the carbonization of alkoxy group (250–350 °C). The exothermic combustion of carbon occurs in the range of 350–450 °C. Due to the very sluggish and complex crystallization path previously deduced [12], DTA measurements on the calcined gels (Si-B-Zr) yielded virtually no observable endo- or exothermic peaks attributable to zirconia (t and m) crystallization at about 950 and 1350 °C respectively. The substantial weight loss in the TGA curve is associated with a removal of large quantities of water or organic materials.

A representative infrared spectrum of gels (sample c and f) studied is illustrated in Fig. 6. The broad ab-

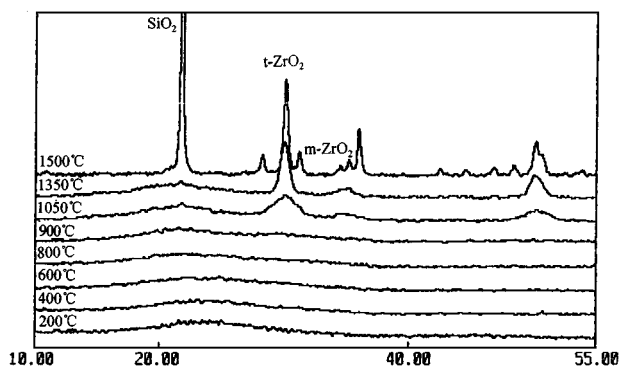


Figure 3 XRD results of the sample c.

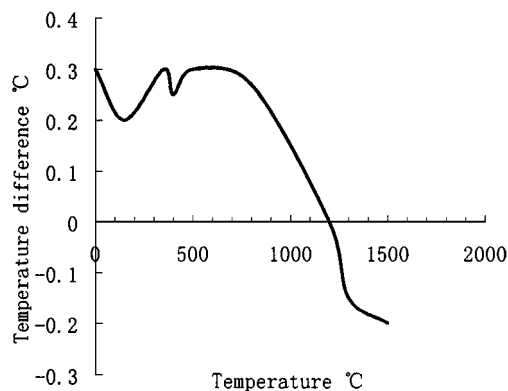


Figure 4 DTA curve of the prepared sample f.

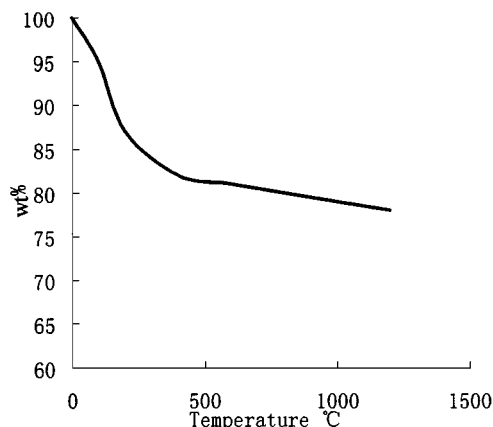


Figure 5 TGA curve of the prepared sample f.

sorption band ranging from 3700–3100 cm⁻¹ arises from the stretching vibration of hydroxyl groups. The band at around 1640 cm⁻¹ is owing to the deformation

TABLE II Crystallization of gel sample

Temperature/°C	a	b	c	d	e	f
≤850	A	A	A	A	A	A
950	A	A	TZ _t	A	A	TZ _t
1050	A	TZ _t	TZ _w	A	TZ _t	TZ _t
1200	A	TZ _w	TZ _w	A	TZ _w	TZ _w
1350	A	TZ _m	TZ _m + MZ _t	A	TZ _w + MZ _t	TZ _w + MZ _t
1500	C _w	TZ _s , C _s	TZ _s + C _s + MZ _w	A	TZ _w + MZ _t	TZ _w + MZ _t
Amount of crystalline at 1500 °C	1~5%	>50%	>80%	0	<1%	1~3%

A = amorphous; TZ, MZ = tetragonal and monoclinic ZrO₂, respectively C = cristobalite; t = trace, w = weak, m = medium, s = strong.

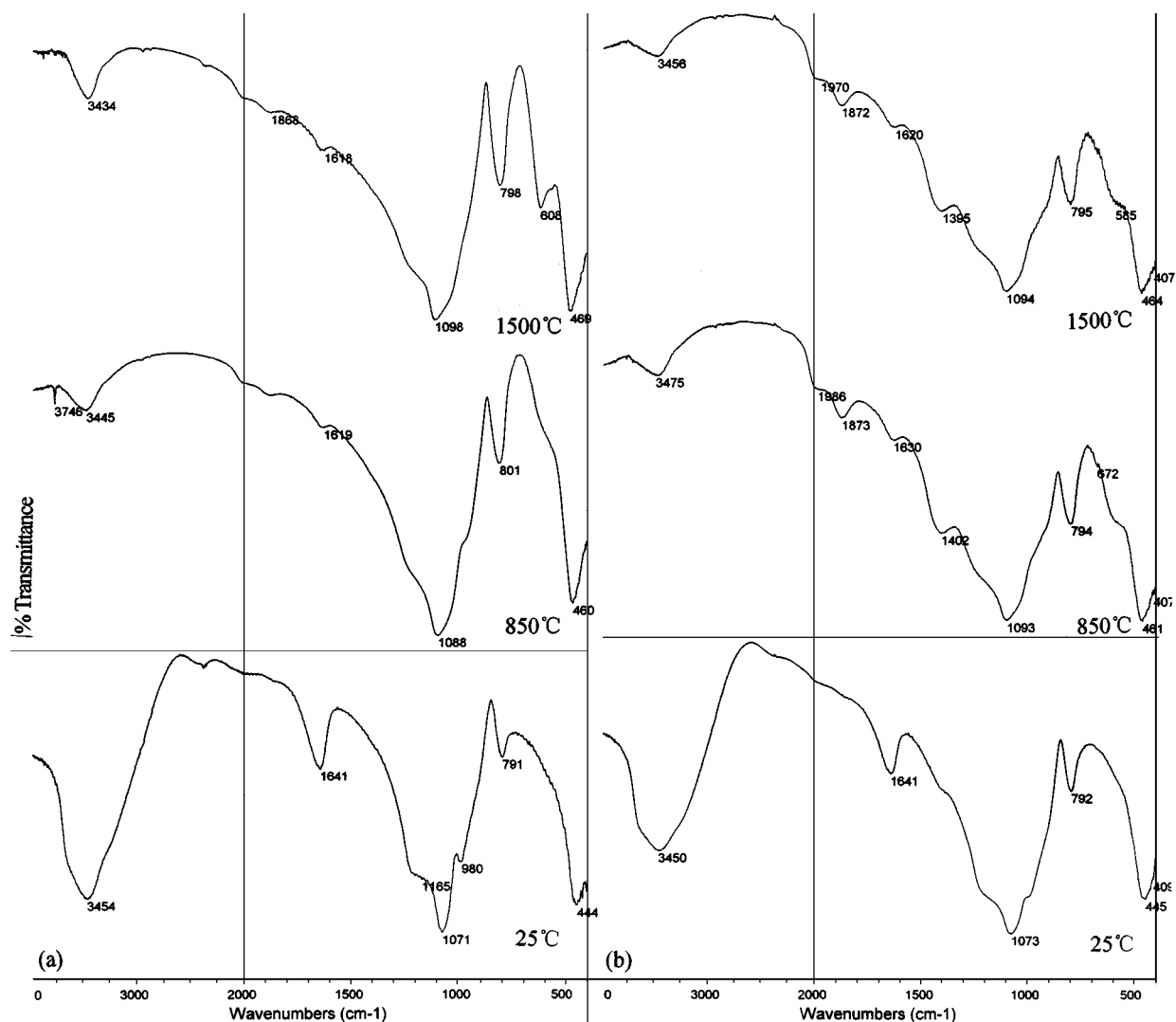


Figure 6 Infrared spectra of (a) sample c and (b) sample f at 25, 850, and 1500 °C, respectively.

vibration of water [13]. Si-O stretching vibrations are reported to occur in around 1180, 1080, 750, 640, and 608 cm^{-1} . Ring structures of Si-O-Si bonds vibrate at around 800 cm^{-1} . The absorption band caused by hydroxyl groups is observed to reduce in intensity as the gels are heated to higher temperature, indicating a continuous desorption of hydroxyl ions from the gel structure. All of these are shown in Fig. 6a and b.

During this desorption process mentioned above, the chemically bonded water is released, giving rise to the Si-O-Si and Si-O-B bonds at the expense of the Si-OH and Si-OR groups, which is confirmed by the fact that the absorption band near 920 cm^{-1} and attributed to the Si-O-B stretching vibration [9] appears at 850 °C up to 1500 °C at the expense of the Si-OH band [8], see Fig. 6b. On the other hand, Fig. 6b shows that the Si-O-B vibration band is observed to grow with increasing heat-treatment temperature, and the band near 680 cm^{-1} marking the Si-O-B deformation vibration also increases with treatment temperature and moves towards greater wave-numbers, indicating a reinforcement of the bonds. Similarly, the absorption bands due to Si-O and Si-O-Si bonds are observed to shift to higher wave numbers with an increasing of heating temperature, inferring the strengthening of these bonds in the

gel structure, see Fig. 6a and b. The band representing B-O stretching vibration at about 1400 cm^{-1} appears with clear outline [8], shown in Fig. 6b, if the heat treatment temperature is increased. Enhancement of band intensity with temperature is explained through B-OH group incorporation into borosilicate phase, during which Si-O-B bonds are progressively formed. This process will be discussed later.

As would be expected, the concentrations of Si-O and Si-O-Si groups (see Fig. 6) decrease with the increasing of zirconium ion that is introduced into the silica network of the gel [14], in comparison with the IR spectrum of the pure SiO_2 and $\text{SiO}_2\text{-B}_2\text{O}_3$ gels shown in ref [10], which means that, with the increasing of zirconium wt pct, the crystallization temperatures of $\text{SiO}_2\text{-ZrO}_2$ and $\text{SiO}_2\text{-ZrO}_2\text{-B}_2\text{O}_3$ gel systems decrease obviously (see Table II).

3.3. The undercoolings of the DD3 single crystal superalloy melt in the Si-Zr-B coating mold

In this coating mold, large undercoolings 100, 120, 140 K were obtained after pouring the purified melt into it, and highly developed dendrite was formed. The

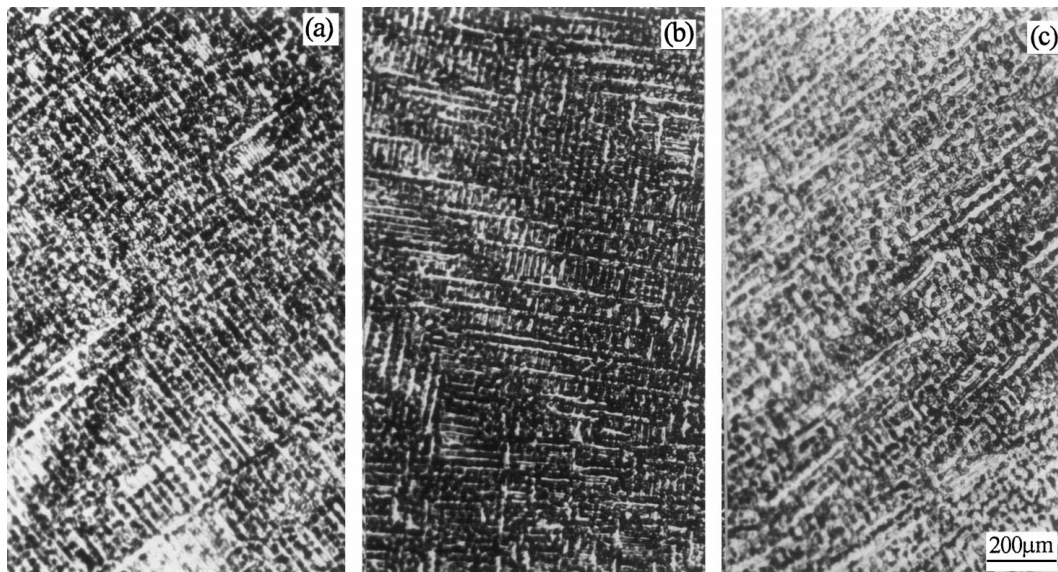


Figure 7 The dendrite structure in the non-catalytic nucleation coating mold at undercoolings of (a) 100 K, (b) 120 K, and (c) 140 K, respectively.

microstructure corresponding to undercoolings were shown in Fig. 7.

4. Discussions

4.1. Stability and persistence of gel-derived metastable zirconia

The result presented above clearly indicates that metastable zirconia particles can be stabilized in a gel-derived glass matrix. The phase transformation from metastable *t*- to *m*-ZrO₂ usually observed in zirconia powders in the range of 600–1000 °C [15], was not observed in this sample, which implies that the same ZrO₂ particles are trapped inside SiO₂ particle, and apparently, *t*-ZrO₂ is found first, then *a*-SiO₂ is deposited and covers the *t*-ZrO₂ particles. The stabilization of *t*-ZrO₂ particles obtained either by precipitation or calcination at various temperature up to 1000 °C was explained by Carvie [16] in terms of a higher surface energy for the stable monoclinic form with respect to that of the metastable, tetragonal one, which means that, because the *t*-*m* transformation involves a positive change of volume, it is appealing to consider that the compressive stress due to the high-melting, low-expansively, covalently bonded strong matrix of SiO₂ is not readily overcome by the low levels of expansion stress of small particles of *t*-ZrO₂ resulted from the volume change in phase transformation (transformation volume). Thus a critical size is required for the *t*-ZrO₂ particle (depending upon the composition and/or temperature), so that the SiO₂ encasement is broken up due to stresses caused by the transformation volume. According to Carvie, the tetragonal zirconia particles can not exist at room temperature for a crystallite size larger than 30 nm, i. e. the inhibition of this phase transformation could be ascribed to a blocking effect of silica, which would hinder the growth of zirconia particles, keeping them below their critical size (30 nm) [17]. The growth and coarsening of metastable zirconia crystallites, as illustrated in Figs 1 and 2, infer that these process occur very slowly, probably via a diffusion-controlled mech-

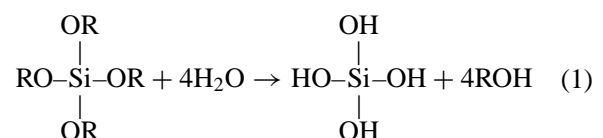
anism. Similar results were also reported by Forgherazi and Znzo [18].

4.2. The effect of boron in inhibiting crystallization of Si-B and Si-Zr-B systems

It was shown clearly in Table II, that obvious difference of crystallization temperature and crystalline amount exists between sample a, b, c and sample d, e, f with addition of B₂O₃. In binary or multicomponent glass, B₂O₃ usually appears as [11, 19]: (1) chain or layer structure formed by [BO₃] trihedral with charge neutrality, (2) glass network structure formed by combination and linkage of [BO₄]⁻ tetrahedral with negative ion and other tetrahedral or trihedral with charge neutrality. When metal cations exist in glass structure, they surround the [BO₄]⁻ tetrahedral to keep the charge neutrality.

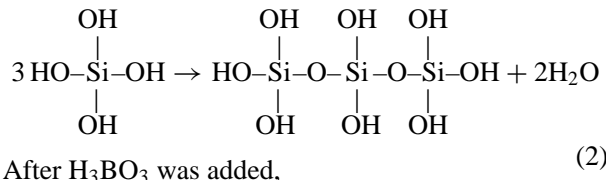
The decisive factors influencing the coordination condition are [10, 19]: (1) the content and ability in supplying free oxygen ion of alkali and alkali-earth metal, (2) the content of SiO₂. Usually, in the R₂O-B₂O₃-SiO₂ systems with low B₂O₃ content, the content of SiO₂ is sufficient, so whether or not the B³⁺ locates in [BO₄]⁻ tetrahedral is decided by the content of free oxygen ion supplied by alkali or alkali-earth metal. The formation process of Si-O-B ([BO₄]⁻) as mentioned above is shown in the following equations. The [BO₄]⁻ tetrahedral is the product in the process of hydrolyzing-condensation of TEOS:

Firstly,

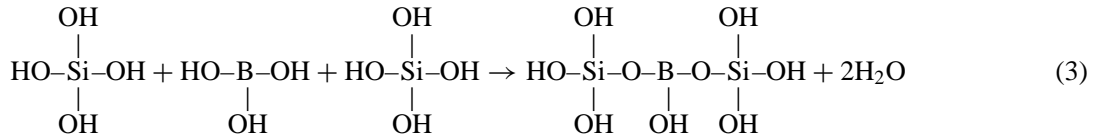


Where, R stand for C₂H₅

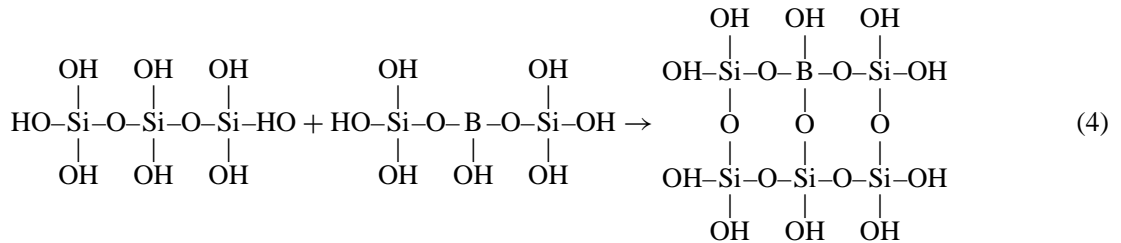
Then,



After H_3BO_3 was added,



Then, the condensational reaction between products of Equations 2 and 3 takes place.



In $\text{Na}_2\text{O}-\text{B}_2\text{O}_3-\text{SiO}_2$ system, when B^{3+} transformed from BO_3 trihedral to $[\text{BO}_4]^-$ tetrahedral, the primitive broken bonds (Si-O) owing to the addition of Na^+ into network were attached by $[\text{BO}_4]^-$ tetrahedral, leading to a three dimensional network. Therefore, the oxygen ion linked previously by Si-O bond is stabilized by B-O and Si-O bonds together, and because of the smaller volume of $[\text{BO}_4]^-$ than that of $[\text{SiO}_4]$, the density and strength of $\text{SiO}_2-\text{B}_2\text{O}_3-\text{Na}_2\text{O}$ glass network increases, when the ratio of $\text{Na}_2\text{O}/\text{B}_2\text{O}_3 > 1$. In $\text{SiO}_2-\text{ZrO}_2$ system, however, a large action force exists between oxygen ion and metal cation Zr^{4+} , compared with that between oxygen ion and metal cation Na^+ . In addition, Zr^{4+} is not a network-forming ion, but a network-modifying ion, so the addition of Zr^{4+} into SiO_2 matrix will give rise to the network-breaking, and aggregation, which means that Zr^{4+} makes oxygen ion arrangement around itself according to its coordination number. After B_2O_3 was added into $\text{SiO}_2-\text{ZrO}_2$ matrix, the formation of $[\text{BO}_4]^-$ tetrahedral could alleviate the effect of aggregation and link the broken bond (Si-O- -Si-O), thus making the total silica network much denser and stronger. As shown in Fig. 6b, the B-O band moves towards lower wave-number and grows in intensity with the increasing of temperature, the initial appearance of this band at higher wave-number indicates that, at lower temperature, the non-bridge B-O bands are predominant, but the fact that there does not appear any absorption band around 720 cm^{-1} (B-O-B deformation vibration) suggests that the B_2O_3 incor-

porate into the network to form Si-O-B links, but not B-O-B bonds, as has been pointed out in the reference [8]. Therefore, in the process of temperature increasing shown in Fig. 6b, the Si-O-B band ($[\text{BO}_4]^-$) formed progressively. As a result, the crystallization trend of $\text{SiO}_2-\text{ZrO}_2-\text{B}_2\text{O}_3$ system decreases with the addition of B_2O_3 .

5. Conclusion

The preparation of glass containing metastable t- ZrO_2 from gels in the ternary system of $\text{SiO}_2-\text{ZrO}_2-\text{B}_2\text{O}_3$ was investigated. The data obtained from DTA-TGA, XRD and IR spectrum explain the following situations:

(1) The crystallization of t- ZrO_2 and the phase transformation between t- and m- ZrO_2 are diffusion-controlled processes.

(2) With regard to the structure of the gels, the fact is especially relevant that the $\text{SiO}_2-\text{ZrO}_2$ and $\text{SiO}_2-\text{ZrO}_2-\text{B}_2\text{O}_3$ systems do not devitrify or crystallize in the experimental heat-treatment temperature range up to $850 \text{ }^\circ\text{C}$, which indicates that the SiO_2 matrix could retard the crystallization of t- ZrO_2 and block the transformation from t- to m- ZrO_2 .

(3) After holding the $\text{SiO}_2-\text{ZrO}_2$ and $\text{SiO}_2-\text{ZrO}_2-\text{B}_2\text{O}_3$ gel systems at $1500 \text{ }^\circ\text{C}$ for 30 min, there appear up to 3% crystallite in the $\text{SiO}_2-\text{ZrO}_2-\text{B}_2\text{O}_3$ system and up to 80% in the $\text{SiO}_2-\text{ZrO}_2$ system, respectively. All of these suggest that the presence of B_2O_3 make the silica network denser and stronger, thus inhibiting the silica crystallization trend.

(4) The result that high undercooling of the DD3 single crystal superalloy melt was obtained in the Si-Zr-B coating mold demonstrate that this coating have ideal structure stability and noncatalytic nucleation property.

Acknowledgement

The authors are grateful to the national Nature Science Foundation and the aeronotic science foundation of China for the financial support under grant NO. 59871041 and NO. 98H53093.

References

1. J. F. LI, Y. L. LU and G. C. YANG, *Progress in natural Science* **7**(6) (1997) 736.
2. F. GARTNER, A. F. NORMAN and A. L. GREER *et al. Acta Mater* **45**(1) (1997) 51.
3. X. F. GUO, Y. L. LU and G. C. YANG, *Chinese Journal of Materials Research* **12**(6) (1998) 598.
4. A. LUDWIG, I. A. WANGER and J. LAAKMANN, *et al., Mater. Sci. Eng.* **A178** (1994) 299.
5. K. H. SUN, *J. Amer. Ceram. Soc.* **56** (1947) 639.
6. A. MAKISHIMA, H. OOHASHI, K. KOTANI and N. ENDO, *J. Non-Cryst. Solids* **42** (1980) 545.
7. C. A. SORRELL and C. C. SORRELL, *J. Amer. Ceram. Soc.* **60** (1977) 495.
8. J. PHALIPPOU, M. PRASSAS and J. ZARZYCKI, *J. Non-Cryst. Solids* **48** (1982) 17.
9. R. JABRA, J. PHALIPPOU and J. ZARZYCKI, *Rev. Chim. Min.* **16** (1979) 245.
10. X. F. GUO, PhD thesis, Northwestern Polytechnical University, China, 1999.
11. F. LIU, X. F. GUO and G. C. YANG, to be published.
12. J. S. HARTMAN, R. L. MILLARD and E. R. VANCE, *J. Mater. Sci.* **25** (1990) 2785.
13. J. FRIPIAT and A. JELLI, *Congr. Int. Du Verre, Bruxelles* **1** (1968) 14.
14. I. M. LOW, PhD thesis, Monash University, Australia, 1986.
15. M. OCANA, V. FORNES and C. J. SERNA, *Ceram. Int.* **18** (1992) 99.
16. R. C. GARVIE, *J. Phys. Chem.* **69** (1965) 1238.
17. V. S. NAGARAJAN and K. J. RAO, *J. Mater. Sci.* **24** (1989) 2140.
18. G. FAGHERAZZI and S. ENZO, *J. Mater. Sci.* **15** (1980) 2693.
19. F. X. GAN, "Optical Glass" (Science Publishers, 1982).

Received 16 December 1999

and accepted 23 February 2000